Biophysical Journal
Article

Biophysical Society

A Microfluidic Platform for Real-Time Detection and Quantification of Protein-Ligand Interactions

Therese W. Herling,[1] David J. O'Connell,[2] Mikael C. Bauer,[3] Jonas Persson,[3,5] Ulrich Weininger,[4] Tuomas P. J. Knowles,[1,*] and Sara Linse[3,*]

[1]Department of Chemistry, University of Cambridge, Cambridge, United Kingdom; [2]School of Biomolecular and Biomedical Science, University of College Dublin, Dublin, Ireland; [3]Department of Biochemistry and Structural Biology and [4]Department of Biophysical Chemistry, Lund University, Lund, Sweden; and [5]Department of Immunology, Genetics and Pathology, Uppsala University, Uppsala, Sweden

ABSTRACT The key steps in cellular signaling and regulatory pathways rely on reversible noncovalent protein-ligand binding, yet the equilibrium parameters for such events remain challenging to characterize and quantify in solution. Here, we demonstrate a microfluidic platform for the detection of protein-ligand interactions with an assay time on the second timescale and without the requirement for immobilization or the presence of a highly viscous matrix. Using this approach, we obtain absolute values for the electrophoretic mobilities characterizing solvated proteins and demonstrate quantitative comparison of results obtained under different solution conditions. We apply this strategy to characterize the interaction between calmodulin and creatine kinase, which we identify as a novel calmodulin target. Moreover, we explore the differential calcium ion dependence of calmodulin ligand-binding affinities, a system at the focal point of calcium-mediated cellular signaling pathways. We further explore the effect of calmodulin on creatine kinase activity and show that it is increased by the interaction between the two proteins. These findings demonstrate the potential of quantitative microfluidic techniques to characterize binding equilibria between biomolecules under native solution conditions.

INTRODUCTION

Weak and transient protein-ligand interactions are essential for cellular signaling and regulatory pathways. A quantitative understanding of this complex network of noncovalent interactions is key to providing fundamental insights into the molecular processes underpinning biological function. A range of biophysical methods have been developed to probe noncovalent protein interactions and the formation of protein complexes (1–6). However, studies of these processes may be limited by requirements with respect to the quantity of the sample, molecular size, persistence of the labile complexes during the measurement, and resistance of dynamic species to dissociation during sample preparation.

Surface-based techniques are widely used to detect and characterize protein-protein interactions. Such methods, including surface plasmon resonance (SPR), are convenient, as they can be automated, but they require the attachment of one of the binding partners to a functionalized surface, a process which can affect the binding equilibrium (4,7). Gas phase methods avoid the use of surfaces, and elegant studies of protein complex formation have been made using this approach (2,6), but it can be complex and costly to implement. The development of complementary solution-based techniques to investigate proteins and their interactions is therefore desirable.

Traditional assays in bulk solution impose limitations as to the concentrations and amounts of sample required, as well as the timescale of the measurement, factors that limit the range of affinities and rate constants that can be discovered by each technique. Furthermore, to achieve a broad understanding of the biophysical basis of protein-ligand binding, the determination of absolute values for the parameters defining these interactions is necessary. Optical microscale assays can readily be applied to a wider size range of sample molecules and typically require considerably less sample material than bulk-solution techniques (8,9). Thermophoretic measurements of differential analyte migration in a temperature gradient are examples of such miniaturization (10). In this study, we address these challenges and present a general method for the quantitative study of noncovalent protein interactions under native solution conditions. To achieve this objective, we used a microfluidic

Submitted November 30, 2015, and accepted for publication March 25, 2016.

*Correspondence: tpjk2@cam.ac.uk or sara.linse@biochemistry.lu.se

Editor: Rohit Pappu.

http://dx.doi.org/10.1016/j.bpj.2016.03.038

platform to measure the absolute value of a key parameter characterizing the solvated proteins, the electrophoretic mobility, μ_e. By measuring an absolute value for a physicochemical parameter characterizing the analyte we were able to compare results directly between solution conditions. Furthermore, microfluidic assays allow characterization of sample molecules of a wide range of dimensions and concentrations. These are advantageous features for the study of noncovalent complex formation by proteins.

The electrophoretic mobility reports on the size and charge state of the migrating species, and can therefore be exploited to differentiate between isolated protein molecules and protein complexes (11). Free-flow electrophoresis, where an electric field is applied perpendicular to the direction of flow, and capillary electrophoresis, where the field is parallel to the direction of flow, have both been adapted to a microfluidic format (12,13). Unlike native gel electrophoresis or size-exclusion chromatography, these methods do not require sample molecules to pass through a matrix, which could introduce additional variables to the measurement, but achieve spatial separation of sample molecules in free solution.

The electrophoretic mobility of molecular species can be measured by both free-flow electrophoresis and capillary electrophoresis, with the latter requiring the use of a mobility standard (13–16). Whereas protein-ligand interactions have been probed by capillary electrophoresis (14), many microfluidic free-flow electrophoresis studies have focused on the qualitative separation of sample molecules (17). Gradient microfluidic free-flow electrophoresis has been applied to probe DNA-protein binding through near-continuous observation of the equilibrium distribution at a large number of target concentrations. In this case, the formation of bubbles within the microfluidic device resulted in a variable electric field and thereby in fluctuations in the observed sample deflection (18). In this article, we demonstrate the use of a microfluidic free-flow electrophoresis assay, where the electric field is quantified, thereby enabling the sample electrophoretic mobility to be quantified and compared between solution conditions (15,16).

We apply the microfluidic platform shown in Fig. 1, *A* and *B*, to shed light on the ligand-binding equilibria of calmodulin. Many diverse and vital signaling pathways, including the control of heart function, cell death by apoptosis, memory, and learning are activated in response to variation in the intracellular concentration of Ca^{2+}, and the protein calmodulin is at the focal point of calcium-mediated signaling (19,20). We therefore chose to elucidate the ion-dependent ligand binding of this protein as a representative model of protein-protein interactions in signal transduction.

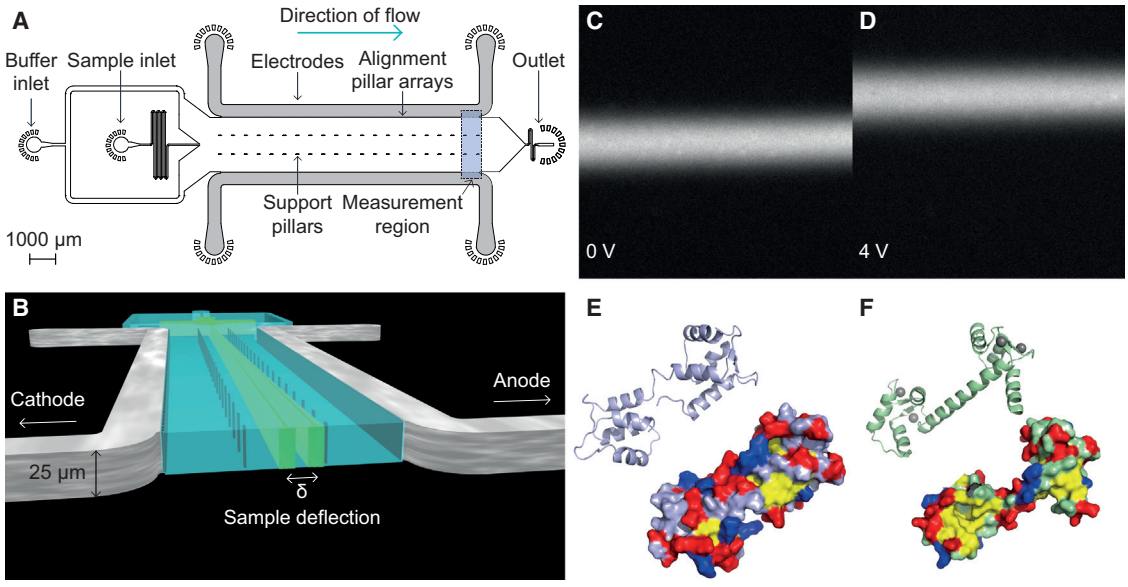

FIGURE 1 Experimental design. (*A*) The design of the microfluidic free-flow electrophoresis device used in this study. Integrated metal electrodes are shown in gray. Inlets for the sample and buffer are indicated. Support pillars for the channel ceiling and the pillar array utilized for the electrode integration and alignment are also shown. The sample deflection is measured at the end of the electrophoresis channel (*blue shaded area*). (*B*) A pseudo-three-dimensional representation of the device showing a cross section of the main electrophoresis channel. Upon application of an electric potential, the sample is deflected from its path at the center of the channel. The scale bar refers to the vertical dimension. (*C*) Fluorescence image of 1 μM calmodulin in the buffer containing EDTA at 0 V. (*D*) Fluorescence image of 1 μM calmodulin in the buffer containing EDTA at an applied potential of 4 V. The negatively charged protein is deflected toward the anode. (*E*) The structure of calmodulin in the absence of Ca^{2+} shown as a ribbon diagram (*top*) and as a surface plot with hydrophobic residues (isoleucine, leucine, phenylalanine, and methionine) in yellow, acidic residues in red, and basic residues in blue (PDB: 1CFD) (22). (*F*) The structure of calmodulin with four Ca^{2+} (*gray spheres*), chelated by the four EF-hands, can be seen in the ribbon diagram (*top*), whereas the surface representation (*bottom*) reveals the exposure of two hydrophobic patches upon Ca^{2+} binding (PDB: 3CLN) (23).

Calmodulin is a small, 16.7 kDa, ubiquitously expressed signaling protein with >300 reported interaction partners (see (21) and references therein). It contains four calcium-binding helix-loop-helix motifs, called EF-hands (Fig. 1, *E* and *F*) (22–24). These are present as EF-hand pairs forming two globular domains connected by a flexible linker. Binding of Ca^{2+} to the calmodulin EF-hands occurs with pairwise cooperativity, leading to conformational changes, as seen in Fig. 1, *E* and *F* (22,23,25). These conformational changes result in the exposure of hydrophobic residues, in many cases increasing the binding affinity of calmodulin for target proteins (Fig. 1 *F*) (4,20,26). The flexible central linker of calmodulin allows the protein to wrap around the target segment of a binding partner (27–31). The prevalence of flexible methionine side chains at the hydrophobic patches of Ca^{2+} -bound calmodulin and the adaptable fold underlie its promiscuity in target recognition (32–34).

The microfluidic free-flow electrophoresis method presented in this article can be applied as a general method for the detection and characterization of protein-ligand interactions. This technique does not rely on specific properties of the sample molecule and is thus ideally suited for the investigation of newly discovered protein-ligand interactions. We used the electrophoretic binding assay to validate and explore the calcium dependence of calmodulin binding to creatine kinase (35,36), which we have identified in this study as a ligand in a surface-based protein array screen. In a negative control, we did not observe binding to calbindin D_{9k} (37), whereas we did observe binding to a known binding partner, phosphorylase kinase (26,31,38,39). The results of these studies highlight the need for fast nondisruptive assays for the quantitative characterization of protein interactions in solution.

MATERIALS AND METHODS

Microfluidic free-flow electrophoresis measurements

Microfluidic devices were prepared using standard soft lithography methods (40). Electrodes were integrated as described in the Supporting Material and previously reported (15). Fluorescence images for the electrophoresis experiments were recorded using a charge-coupled-device camera (Photometrics Evolve 512, Photometrics, Tucson, AZ) through inverted optics (Observer D1, Zeiss, Oberkochen, Germany). Electrophoresis measurements for each target protein were performed under two sets of buffer conditions, 5 mM Tris-HCl, pH 8.0, with either 0.1 mM $CaCl_2$ or 0.1 mM EDTA to chelate any trace calcium ions. Unless otherwise stated, buffer solutions were prepared using chemicals of analytical grade purchased from Sigma (St. Louis, MO). Measurements were performed for a range of binding partner/calmodulin ratios depending on the observation of a plateau in the measured electrophoretic mobility.

To track calmodulin within the microfluidic device, the protein was labeled with Alexa488, as described in the Results and the Supporting Material. The sample was introduced at the center of the fluid flow within the electrophoresis channel. The sample stream would span the vertical direction of the channel, as illustrated in Fig. 1 *B*. Sample molecules were transported past the electrodes by the flow through the channel (Fig. 1 *A*). Upon the application of an electric field across the electrophoresis channel, the sample molecules migrated perpendicular to the direction of flow according to their electrophoretic mobility.

Fluorescence image acquisition, the application of an electric potential, and current measurements by a multimeter (Agilent Technologies, Santa Clara, CA) were triggered through a lock-in amplifier (Stanford Research Systems, Sunnyvale, CA). Experiments were performed at room temperature, 23°C. The flow rate through the device was set to 500 μL h^{-1} and controlled by withdrawal through the outlet using a glass syringe (Hamilton, Bonaduz, Switzerland) and a syringe pump (neMESYS, Cetoni, Korbussen, Germany) (Fig. 1 *A*). The lower flow velocities at the edges of the microfluidic channel were taken into consideration, and the average flow rate in the region of the channel explored by the sample was evaluated to be 510.9 μL h^{-1} (41). This value was used in calculations of the residence time of 3.4 s and v_d.

Four repeats of a voltage ramp of 0–4 V at 0.5 V intervals were applied for each sample. After each change in the applied potential, there was a pause between image acquisitions, so that the imaged sample had only been exposed to one voltage while traveling through the electrophoresis channel. The applied voltage range was adjusted so as to achieve significant sample deflection (Fig. 1, *C* and *D*), and electrolysis products were removed by the flow through the channel and thus prevented from accumulating beyond their solubility limit. The mean displacement of the sample signal was measured at the end of the separation channel (see Fig. 3 *C*). The electrophoresis channel was 10,000 μm long, with a height of 25 μm and a width of 2100 μm, and an array of support pillars were placed in the wide channel (Fig. 1, *A* and *B*). Each electrophoretic mobility measurement consumed 1.6 μL of sample. For a 1 μM solution of calmodulin, this volume corresponds to 1.6 pmol of protein. To fit three free parameters, at least nine electrophoretic mobility measurements would be required.

Calibration of the cell constants and buffer conductivities were also performed using a lock-in amplifier (15). Detailed descriptions of the calibration procedure and the subsequent determination of the electric field can be found in (15). Using Ohm's law, the effective voltage drop, $V_{effective}$, across the solution was determined from the buffer conductance and the measured current. The electric field corresponding to each current measurement was then found by dividing $V_{effective}$ by the distance between the electrodes (see Fig. 3 *D*). The electrophoretic mobilities of the solvated proteins were determined by a linear fit to v_d against E (see Fig. 4). Electrophoresis data analysis was performed using software written in Python.

Cloning, expression, and purification of creatine kinase

The creatine kinase B gene was purchased from the Arizona State University clone collection and cloned into the PetSac vector using standard polymerase chain reaction and cloning techniques. The protein was expressed in *Escherichia coli* strain BL21 Des3 pLysS star in lysogeny broth. The protein was purified from inclusion bodies. These were isolated by probe sonication of the cell pellet from 2 L of culture in 40 mL 10 mM Tris-HCl and 1 mM EDTA, pH 7.5, for 1.5 min (1/2 horn, maximum output, duty cycle 50%) in a beaker surrounded by ice-water slurry, followed by centrifugation for 10 min at 18,000 × *g* at 4°C. The pellet was solubilized in 8 M urea, 10 mM Tris-HCl, and 1 mM EDTA, pH 7.5. The protein was then purified by anion exchange chromatography on a 3.4 × 10 cm DEAE cellulose column equilibrated in 10 mM Tris-HCl and 1 mM EDTA, pH 7.5, and eluted by a linear salt gradient from 0 to 300 mM NaCl in 10 mM Tris-HCl and 1 mM EDTA, pH 7.5, to a total gradient volume of 400 mL. Five-milliliter fractions were collected and examined by ultraviolet absorbance at 280 nm and by sodium dodecyl sulfate polyacrylamide gel electrophoresis. Fractions containing creatine kinase were combined, concentrated, and further purified by size-exclusion chromatography on a Superdex 200 column equilibrated and eluted in 10 mM Tris-HCl, 1 mM EDTA, and 50 mM NaCl, pH 7.5. Purity was confirmed by agarose gel electrophoresis in EDTA and by sodium dodecyl sulfate polyacrylamide gel electrophoresis.

Calmodulin-binding protein profiling on ProtoArrays

For the protein array screen, ProtoArray slides (Invitrogen, Carlsbad, CA) were blocked through incubation in 1% w/v skimmed milk powder dissolved in phosphate-buffered saline containing 1 mM dithiothreitol, 0.1% v/v Tween20, and 50% v/v glycerol, pH 7.5 for 1 h and then washed five times in Tris-buffered saline and 0.1% v/v Tween20, pH 7.5. The ProtoArray was then incubated with 1 μM Alexa546-labeled calmodulin in 50 mM Tris-HCl, 150 mM NaCl, 0.1% v/v Tween20, pH 7.5, and either 1 mM $CaCl_2$ or 1 mM EDTA for 90 min, followed by five 5 min washes with the same buffer without calmodulin. Before imaging, the slides were rinsed in deionized water. Imaging was performed using a Genepix 4000B scanner (Axon Instruments, Sunnyvale, CA) with excitation at 532 nm and 635 nm, the latter for detection of red-labeled control proteins spotted on the array to guide the analysis.

Creatine kinase activity by NMR spectroscopy

All experiments were performed at 37°C in 10 mM Tris-HCl, 150 mM KCl, 100 μM $MgCl_2$, 100 μM $CaCl_2$, and 10% v/v D_2O, pH 7.5, at a static magnetic field strength of 14.1 T. Series of one-dimensional ^{1}H NMR spectra were recorded over time at several concentrations (1–37 mM) of creatine phosphate and ADP in the presence of 0.5 μM creatine kinase with and without 0.5 μM Ca^{2+} -loaded calmodulin (see Fig. 5). Creatine phosphate and ADP concentrations were altered in parallel. Decay of creatine phosphate (resonances at 3.94 and 3.04 ppm) and buildup of creatine (3.90 and 3.01 ppm) were monitored over time and converted into initial rate constants. Neither ADP nor ATP displayed any signals that were isolated enough for quantification. Doubling of the calmodulin concentration resulted in virtually the same kinetics. The auto reaction was studied without the enzyme present and found to be insignificant during the experimental time. Spectra were processed and analyzed with NMRPipe (42). Michaelis-Menten kinetics were fitted to models without (in the presence of calmodulin) and with a Hill parameter (without calmodulin) to account for allosteric effects.

RESULTS

We combined microfluidic and electrical components to generate a microfluidic platform for protein ligand-binding assays. To establish a well-defined electric field, we integrated self-aligning three-dimensional (3D) electrodes into microfluidic devices (Fig. 1 *A*) (15,16,43). Using these microfabricated electrodes, we were able to perform quantitative free-flow zone electrophoresis in aqueous solutions (Fig. 1, *A* and *B*) (15,16). Upon application of an electrical potential, the sample molecules migrated perpendicular to the direction of the fluid flow according to their electrophoretic mobility, as shown in Fig. 1, *B–D*.

An S17C variant of calmodulin was generated using site-directed mutagenesis. Residue S17 has been identified at the surface of calmodulin-ligand complexes in previous studies (44). Fluorophore-labeled S17C variants have also been used successfully in FRET studies of calmodulin conformational changes (44) and protein array screens (21). To visualize calmodulin in the experiments, the protein was labeled at position 17 with Alexa488 for the electrophoresis measurements or Alexa546 for the protein array screen. Crucially, the target proteins were unlabeled, which enabled us to quantify the extent of ligand binding through the observed mean electrophoretic mobility of calmodulin. With free-flow electrophoresis, analyte sizes ranging from Ångströms to micrometers can be investigated simultaneously. This method is therefore well suited for the study of protein-ligand complex formation.

Surface-based screen for potential calmodulin targets

We sought to explore the potential of microfluidic free flow electrophoresis in the discovery and characterization of new binding targets. To this effect, we performed a protein array screen for calmodulin binding partners (Fig. 2). The protein spots on the array exhibiting the highest signal in the presence of Ca^{2+} are listed in Fig. S1, and those with the highest signal in the absence of Ca^{2+} are listed in Fig. S2. Calmodulin bound to a large number of known interaction partners present in this screen, among which were a number of kinases. Interestingly, the screen also highlighted a number of novel putative targets. Among the previously unknown targets were several creatine kinase isoforms, including the B (brain), M (muscle), and U (mitochondrial) isoforms, observed both in the absence and presence of Ca^{2+}. We chose to further investigate creatine kinase B, as the signal intensity of calmodulin bound to this protein showed the largest apparent calcium dependence in the protein array screen.

Creatine kinase catalyzes the reversible addition of a phosphate ion to creatine (35,36). Abnormalities in creatine kinase metabolism have been associated with an increased risk of heart failure (45). To the best of our knowledge, calmodulin has not previously been reported to interact with this protein. Here, we studied calmodulin binding to

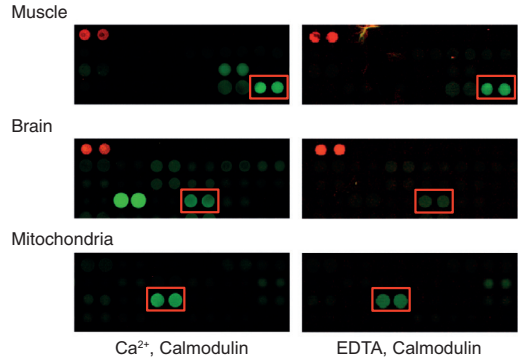

FIGURE 2 Protein array screen for calmodulin-binding proteins. Fluorescence image of the areas of the protein array containing the immobilized brain isoform for experiments performed in the presence of 1 mM Ca^{2+} (*left*) or 1 mM EDTA (*right*). Every protein is present in duplicate dots. The creatine kinase spots have been highlighted with a red bounding box. The very bright spots to the left of the brain isoform in the presence of Ca^{2+} are calcium/calmodulin-dependent protein kinase type 1 (Q14012), a known and highly Ca^{2+}-sensitive binding target of calmodulin.

creatine kinase B using electrophoresis. In these studies, we evaluated the effect of Ca^{2+} on the equilibrium dissociation constant, K_d, of the interaction.

Binding to creatine kinase B is validated in solution by free-flow electrophoresis

The results of the surface-based protein array screen pointed to a potential interaction between calmodulin and creatine kinase B. However, experiments in free solution were required to ascertain that the observed binding to the immobilized substrate was not a nonspecific effect or the result of a change in the conformation of creatine kinase upon surface immobilization. To verify the interaction between calmodulin and creatine kinase in free solution, we performed free-flow electrophoresis using the device shown in Fig. 1 *A*. To minimize the background signal in the fluorescence measurements, we cast the microfluidic devices in black polydimethylsiloxane. A range of electric potential differences were applied across the separation channel, causing the sample molecules to migrate perpendicularly to the direction of flow according to their electrophoretic mobility. The mean deflection, δ, of the labeled calmodulin was recorded (Fig. 3).

In addition to δ, we simultaneously recorded the current, I (Fig. 3 *C*). From measurements of the frequency-dependent admittance, we determined the cell constant for each individual device and the conductivities of the buffers used (15). By combining these measurements with the residence time of the proteins between the electrodes we found the transverse electrophoretic drift velocity, v_d, and the electric field across the separation channel, E (Fig. 3 *D*). The electrophoretic mobility, μ_e, of the sample was given by the slope of v_d against E, $\mu_e = v_d/E$ (Fig. 3 *D*). This parameter reports on the relation between the diffusion coefficient, D, and the charge component, q, defining the migrating molecules:

$$\mu_e = \frac{qD}{k_B T}, \tag{1}$$

where k_B and T represent the Boltzmann constant and the absolute temperature, respectively. The electrophoretic mobility can therefore be exploited to monitor changes in the size and charge of the analyte, for instance, through interaction with other molecules in solution.

The results displayed in Figs. 3 and 4 show a change in the electrophoretic mobility of the fluorescently labeled calmodulin in response to an increasing concentration of unlabeled creatine kinase. This change in μ_e arises from changes in the size and charge of the migrating species, indicating complex formation between calmodulin and creatine kinase (compare Fig. 3, *A* and *B*). At intermediate target protein concentrations, broadening of the fluorescence peak was observed as the sample migrated in the electric field.

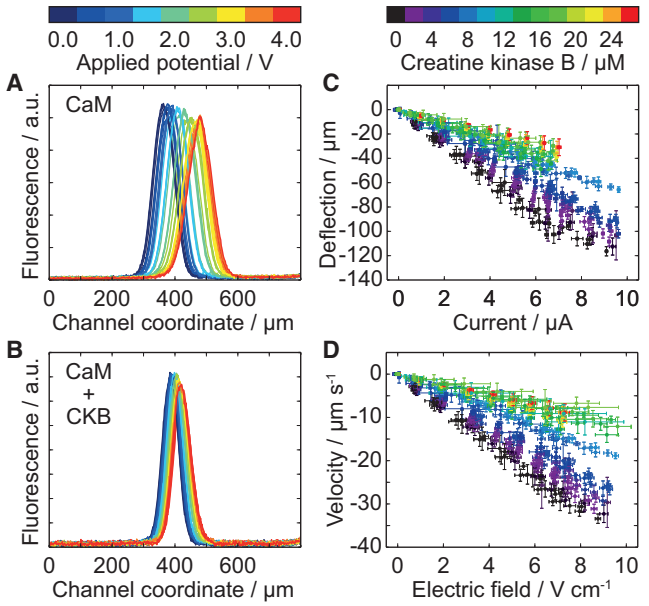

FIGURE 3 Electrophoresis experiments in buffer containing EDTA. (*A*) Sample deflection is monitored via fluorescence. Fluorescence intensity profiles for the isolated protein: 1 μM calmodulin (*CaM*) for four repeats of a voltage ramp. The color bar above (*A*) shows the applied voltage for each profile and applies to (*A*) and (*B*). The profiles are recorded for a cross section of the separation channel. (*B*) Fluorescence intensity profiles for 1 μM labeled calmodulin in the presence of 20 μM unlabeled creatine kinase B (CaM + CKB). (*C*) The measured sample deflection after passing between the electrodes against the measured current for 1 μM calmodulin and 0–27 μM creatine kinase B. Throughout the figure, data points are colored according to the creatine kinase concentration, going from low (*black*) to high (*red*). The color bar applies to (*C*) and (*D*). (*D*) Sample deflection velocity against the electric field across the solution for calmodulin and creatine kinase in the absence of Ca^{2+}.

This observation indicated the coexistence of more than one species with different electrophoretic mobilities, consistent with the presence of isolated calmodulin and calmodulin-target complex. The width of the sample inlet is 50 μm. At the end of the electrophoresis channel, the width of the sample distribution is therefore comparable to δ. Thus, although variation in δ is readily detected, the fluorescence peak does not divide into two peaks. In this study, we combine the accurate determination of the mean sample position with quantification of the electric field, yielding a sensitive analytical assay for the measurement of electrophoretic mobilities without the need for separation of the sample components.

Determination of calcium-dependent equilibrium dissociation constants

In this study, we monitored the electrophoretic mobility of Alexa488-labeled calmodulin as a function of the concentration of unlabeled target protein. The fractional contributions from isolated calmodulin, with an electrophoretic mobility of μ_c, and calmodulin in complex with the target

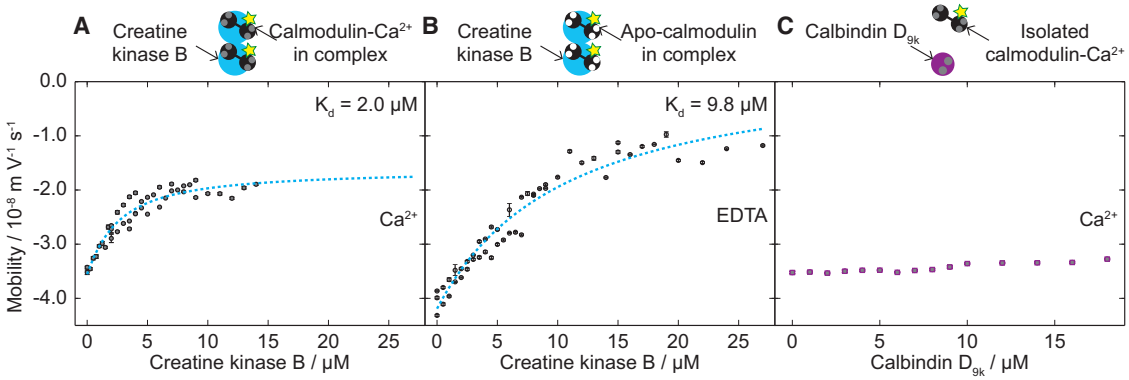

FIGURE 4 Creatine kinase interaction with calmodulin monitored by free-flow electrophoresis. (*A*) The electrophoretic mobility of 1 μM calmodulin shown against an increasing creatine kinase B concentration in the presence of 0.1 mM Ca^{2+}. The dashed line shows a least-squares fit of Eq. 2 to the data. The diagram at the top shows calmodulin (*black*), calcium ions as gray spheres, the label as a star, and creatine kinase (*lighter color*). (*B*) Electrophoretic mobility of 1 μM calmodulin against increasing creatine kinase B concentration in the presence of 0.1 mM EDTA. (*C*) The electrophoretic mobility of 1 μM calmodulin against increasing calbindin concentration in buffer containing 0.1 mM Ca^{2+}. The diagram at the top shows calcium-bound calbindin and calmodulin. To see this figure in color, go online.

protein, μ_{cp}, result in an observed mean electrophoretic mobility, μ_{obs}, of

$$\mu_{obs} = \mu_c \frac{[C]}{C_t} + \mu_{cp} \frac{[CP]}{C_t}. \quad (2)$$

The concentration of free target protein, [P], and the concentration of complex, [CP], can be expressed in terms of the two known total concentrations of calmodulin, C_t, and target protein, P_t, and isolated calmodulin, [C], in the equation for the equilibrium dissociation constant, K_d. This allows the resulting quadratic equation to be solved for [C], as described in the Supporting Material, yielding an expression for [C] in terms of P_t, C_t, and K_d.

We investigated the calcium dependence of calmodulin binding to creatine kinase by performing electrophoresis measurements in 5 mM Tris-HCl containing either 0.1 mM $CaCl_2$ or 0.1 mM EDTA to chelate any residual Ca^{2+} (Fig. 4). Plots of the observed mobility of 1 μM calmodulin as a function of the total concentration of target protein, P_t, are shown in Fig. 4. Inserting the solution for [C] found in the Supporting Material into Eq. 2 allowed us to fit the data with μ_c, μ_{cp}, and K_d as the free parameters.

In agreement with the protein array data, we observed calmodulin binding to creatine kinase B. In the presence of Ca^{2+} in low-ionic-strength buffers, we found the dissociation constant to be 2.0 μM (Fig. 4 *A*). Binding of Ca^{2+} by the four EF-hand motifs of calmodulin leads to conformational changes in calmodulin (Fig. 1, *E* and *F*) (22,23,32) involving exposure of hydrophobic side chains, which results in an increase in the binding affinity for most target proteins (Fig. 1 *F*) (22,23). Indeed, in the absence of free calcium ions, we observed a reduction in the binding affinity, $K_d = 9.8$ μM (Fig. 4 *B*).

In a negative control experiment, we investigated whether the change in μ_{obs} of calmodulin could be the result of nonspecific effects associated with the presence of another protein in solution, for instance, through electrostatic screening by the added protein (46). We chose calbindin D_{9k} as a control system, because although the function of this protein relies on binding of calcium ions, calbindin has not been known to interact with calmodulin. Calbindin D_{9k} contains a pair of EF-hands that enable it to bind and transport two calcium ions (37). In the presence of Ca^{2+} and calbindin at concentrations of 0–18 μM, we did not observe a change in the μ_{obs} of calmodulin (Fig. 4 *C*). In positive control experiments, we detected calmodulin binding to phosphorylase kinase, a well-documented ligand (31,39), with a K_d of 2.2 μM (see Fig. S4).

Direct observation of the fluorescently labeled calmodulin during the electrophoresis experiments furthermore enabled us to confirm the absence of any sample signal with the mobility of the isolated protein, once the electrophoretic mobility had reached a plateau against the concentration of the target protein (Fig. 3 *B*). Calmodulin was found to have a negative μ_e: $-3.5 \pm 0.1 \times 10^{-8}$ m V^{-1} s^{-1} for Ca^{2+}-calmodulin and $-4.1 \pm 0.2 \times 10^{-8}$ m V^{-1} s^{-1} for apocalmodulin. These observations are in agreement with the overall negative charge expected from the amino acid sequence of calmodulin (47). Comparison of the interaction between calmodulin and creatine kinase B in the presence of Ca^{2+} and EDTA reveals that the magnitude of change in μ_e upon binding to creatine kinase B is larger for apocalmodulin than for Ca^{2+}-bound calmodulin. The mobility of the complex approaches comparable values under both sets of conditions; this finding may arise from charge-dependent modulation of pK_a values in the complexes (48).

After the protein array screen and free-flow electrophoresis measurements, we probed the interaction between calmodulin and the target proteins creatine kinase and phosphorylase kinase by SPR (see Fig. 5 *A* and Fig. S3). Calmodulin containing the S17C mutation was site-specifically

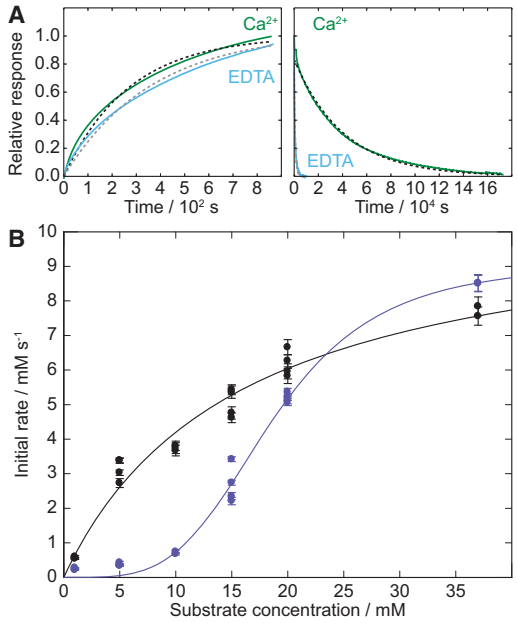

FIGURE 5 Further investigation of the calmodulin-creatine kinase interaction. (*A*) SPR data for 5 μM creatine kinase in buffer containing Ca^{2+} (*dark*) or EDTA (*light*). The association data are shown at left, and the disassociation data are shown at right. The dashed lines represent the fits to determine k_{on} and k_{off} assuming a 1:1 binding event. (*B*) Michaelis-Menten kinetics of 0.5 μM creatine kinase at 37°C in 10 mM Tris-HCl, 150 mM KCl, 100 μM $MgCl_2$, and 100 μM $CaCl_2$ with (*black*) and without (*light*) 0.5 μM Ca^{2+}-loaded calmodulin. The concentrations of creatine phosphate and ADP were altered in parallel, and the initial rate is plotted versus either substrate concentration. The black curve shows the best fits of the Michaelis-Menten model to the data in the presence of calmodulin, whereas the lighter colored curve shows a fit that includes a Hill parameter to account for allosteric coupling between subunits of the enzyme. To see this figure in color, go online.

coupled to the dextrane matrix of the CM5 sensor chips via the thiol side chain of Cys-17, to allow the two domains of calmodulin to move freely relative to one another and cooperate in target binding. A series of creatine kinase B solutions with different concentrations were flowed over CM5 sensor chips with immobilized calmodulin. The SPR experiments were performed both in buffers containing Ca^{2+} and in buffer with EDTA, as shown in Fig. 5 *A*. We obtained values for the rate constants through fits to the association and dissociation data, as detailed in the Supporting Material, yielding $k_{on} = 7.3 \times 10^2\ M^{-1}\ s^{-1}$ and $k_{off} = 2.6 \times 10^{-5}\ s^{-1}$ for creatine kinase B in the presence of calcium and $k_{on} = 3.5 \times 10^2\ M^{-1}\ s^{-1}$ and $k_{off} = 1.1 \times 10^{-3}\ s^{-1}$ in the absence of free Ca^{2+}. Relating these rate constants to the equilibrium dissociation constant provided us with values for the apparent equilibrium dissociation constant of $K_d = 36$ nM for creatine kinase B binding to Ca^{2+}-loaded calmodulin and $K_d = 3.1$ μM for creatine kinase B binding to apocalmodulin on the sensor-chip surface at physiological salt concentration, 150 mM NaCl.

We investigated whether the observed difference in the binding affinity of calcium-bound calmodulin for creatine kinase B between the surface-based experiments and the measurements in solution was due to the changes in ionic strength. To probe the effect of low versus high salt concentrations, we investigated calmodulin binding to creatine kinase B through thermophoresis (see the Supporting Material). The thermophoresis measurements were performed in 0.1 mM $CaCl_2$, 5 mM Tris-HCl, pH 8.0, with either no or 150 mM added KCl. Fitting the data from the thermophoresis measurements in the low-ionic-strength buffer resulted in $K_d = 1.4 \pm 1.8$ μM. In the high-salt buffer, we found the K_d to be 1.7 ± 0.9 μM (see Fig. S5). Thus, when the binding affinity between Ca^{2+} -calmodulin and creatine kinase B was evaluated in free solution, we found the K_d to be the same within error for both low and physiological levels of salt.

Calmodulin binding has an effect on creatine kinase B activity

After the discovery and validation of the interaction between calmodulin and creatine kinase B in solution and on a surface, we addressed the question of whether the binding of calmodulin had an effect on the activity of creatine kinase B. To explore the potential role of calmodulin in modulating the function of creatine kinase B, we monitored the effect of calmodulin on creatine kinase B activity using ^1H NMR. The conversion of ADP and creatine phosphate to ATP and creatine by creatine kinase was monitored via the decay of creatine phosphate signals and buildup of creatine signals. A clear difference in the reaction rate was observed between the presence and absence of Ca^{2+} -loaded calmodulin (Fig. 5 *B*). Over the range of investigated substrate concentrations (ADP and creatine phosphate were altered in parallel between 1 and 37 mM), calmodulin was found to activate creatine kinase and increase the rate of substrate conversion by up to sixfold. Moreover, the influence of calmodulin was more prominent at low substrate concentrations, and the initial rate versus substrate concentration changes from sigmoidal in the absence of calmodulin to hyperbolic in the presence of calmodulin. The latter case could be fitted by standard Michaelis-Menten kinetics ($v_{max} = 11 \pm 1$ mM s^{-1}, $K_M = 15 \pm 2$ mM), but without calmodulin, an additional Hill-coefficient of 3.9 ± 0.4 was needed to obtain a reasonable fit (apparent $v_{max} = 9 \pm 1$ mM s^{-1}, apparent $K_M = 19 \pm 5$ mM). The effects on the apparent values for v_{max} and K_M are in the range of errors, but the difference in allosteric behavior is striking. Typical cellular concentrations at rest are 4 mM ATP, 0.013 mM ADP, 13 mM creatine, and 25 mM creatine phosphate (49). Thus, the activation by calmodulin occurs within a physiologically relevant range of substrate concentrations.

DISCUSSION

To achieve a fundamental understanding of protein function, it is necessary not only to obtain a qualitative knowledge of

the identities of interacting proteins, but also to achieve a quantitative insight into the affinity of the interactions. Microfluidic free-flow electrophoresis provides us with a general tool for the study of protein-ligand binding. Here, we have explored the ligand binding of calmodulin. Through the negative control of calbindin D_{9k}, we were able to demonstrate the specificity of the binding assay. This assay is excellently suited to probe weak interactions between biomolecules, such as the binding of apocalmodulin to creatine kinase, an interaction that was below the cutoff used in the protein array screen. In addition, this solution-based technique is not liable to the artifacts associated with surface-based assays, and the sample can be readily recovered after passing through the microfluidic device.

The interaction between calmodulin and creatine kinase, discovered in this work and quantified using free-flow electrophoresis, suggests a number of implications for human energy metabolism. Indeed, creatine kinase is an important enzyme in tissues that rapidly consume ATP. Creatine phosphate, which has a higher phosphate-transfer potential than ATP, serves as an energy reservoir for the fast generation of ATP in such tissues. The activation of creatine kinase by Ca^{2+}-bound calmodulin may provide a coupling to cellular Ca^{2+} oscillations and signaling. The discovery of a relatively moderate affinity means that these signals can be regulated by calcium oscillations in myocardial and neuronal cells.

In the free-flow electrophoresis study, we determined the K_d values for the equimolar interaction between calmodulin and individual subunits of its binding partners. Creatine kinase B is a homodimer (36), whereas phosphorylase kinase has four γ-subunits (26,31). The measured K_d values for calmodulin binding to creatine kinase B and phosphorylase kinase in the presence of Ca^{2+} in solution are higher than those determined by SPR (see Figs. 2, 4, and S4). However, in the SPR experiments it was not possible to differentiate between a multisubunit protein bound to one or to multiple immobilized calmodulin molecules. Avidity of binding could thus lead to an overestimate of the binding affinity by surface-based assays. Simultaneous dissociation from all the calmodulin molecules would be required for the multimeric binding partner to leave the surface, leading to a reduction in the apparent dissociation rate.

A systematic comparison of protein binding affinity measurements in free solution, in the gas phase, and on a surface, has previously revealed that SPR measurements are liable to report a considerably lower K_d compared with alternative methods (7). Indeed, this report agrees with the findings from our study. Here, we found the same value for the K_d within error through two solution-based methods, whereas we arrived at a higher affinity between Ca^{2+}-calmodulin and creatine kinase B by SPR. Another factor that might contribute to this effect is the common use of a dextran matrix for immobilization, which may lead to enhanced complex formation due to so-called crowding effects or additional avidity effects due to low-affinity binding of the target protein to the dextran (50).

In the case of apocalmodulin, the values for K_d were comparable: 9.8 μM by electrophoresis and 3.1 μM by SPR, whereas, in the presence of calcium, the difference is marked between the surface-based assay, $K_d = 36$ nM, and the experiments in solution, where the measured values for K_d were 2.0, 1.4, and 1.7 μM. These findings suggest that calcium-bound and apocalmodulin interact with creatine kinase through different binding modes (51).

The SPR measurements were performed at physiological salt concentration to minimize unspecific surface effects, whereas microfluidic free-flow electrophoresis can access low-ionic-strength solution conditions. The voltage drop across the electrophoresis channel is proportional to the current and inversely proportional to the conductance of the solution. To achieve readily measurable sample deflections, we have therefore chosen to use low-ionic-strength buffers in these experiments. Even for the low electric potentials applied above, we recorded sample deflections of tens to hundreds of micrometres. The specifications of the optical detection methods influence the resolution of the deflection measurements. In this case, the sample position at a given time can be determined with micrometer or submicrometer precision. The microfluidic device designs can be optimized for use with higher-ionic-strength solutions. For the setup discussed in this work, experiments with salt concentrations on the order of tens of millimolar would be practicable.

Fluorescence images were acquired under steady-state conditions. Lower sample concentrations than those studied above can therefore be accessed by increasing the exposure time, without the risk of photobleaching. The measured current at each step of a voltage ramp would typically be stable to 0.1 μA. The main source of variation in electrophoretic mobility measurements between microfluidic devices originated in the cell constant and buffer conductivity measurements.

CONCLUSIONS

In conclusion, we have developed a general and quantitative approach to probe protein binding equilibria in free solution. The microfluidic free-flow electrophoresis approach presented in this article offers many advantages to the validation and quantification of protein-ligand interactions, including low sample consumption and short analysis time. The method is generally applicable to probe weak and transient interactions between solvated macromolecules. This strategy does not rely on specific solution conditions or exploit particular properties of the sample molecules. We have shown that this electrophoresis method can be applied to detect and characterize specific binding events in solution in a rapid manner. Furthermore, we have quantitatively confirmed the protein microarray

identification of a calmodulin creatine kinase interaction. We found that the binding affinity of calmodulin for creatine kinase B was increased in the presence of calcium ions, and we showed that the catalytic activity of creatine kinase was increased in the presence of calmodulin. The quantitative approach applied here has allowed us to determine μ_e, and from this K_d directly, without the need for complex fitting or reference measurements. This approach therefore has the potential to be applied in a large number of areas of basic and applied research, for example, to measure antibody-antigen binding in drug discovery and for rapid diagnostics. The results presented here therefore open up the possibility of fast and quantitative measurements of protein-protein interactions in free solution under native conditions.

SUPPORTING MATERIAL

Supporting Materials and Methods and five figures are available at http://www.biophysj.org/biophysj/supplemental/S0006-3495(16)30151-5.

AUTHOR CONTRIBUTIONS

T.W.H., D.J.O., U.W., T.P.J.K., and S.L. designed the research. T.W.H., D.J.O., M.C.B., J.P., U.W., and S.L. performed the research. T.W.H., D.J.O., U.W., and S.L. contributed analytical tools. T.W.H., D.J.O., U.W., T.P.J.K., and S.L. analyzed the data, T.W.H., T.P.J.K., and S.L. wrote the manuscript. All authors commented on the manuscript.

ACKNOWLEDGMENTS

We acknowledge financial support from the Biotechnology and Biological Sciences Research Council (T.W.H. and T.P.J.K.), the Newman Foundation, and the European Research Council (T.P.J.K. and S.L.), the Swedish Research Council (S.L., J.P., and M.C.B.), and the Science Foundation Ireland Investigator Programme (D.J.O.).

SUPPORTING CITATIONS

References (52,53) appear in the Supporting Material.

REFERENCES

1. Lomakin, A., D. B. Teplow, and G. B. Benedek. 2005. Quasielastic light scattering for protein assembly studies. *Methods Mol. Biol.* 299:153–174.
2. Benesch, J. L. P., J. A. Aquilina, …, C. V. Robinson. 2006. Tandem mass spectrometry reveals the quaternary organization of macromolecular assemblies. *Chem. Biol.* 13:597–605.
3. Berggård, T., S. Linse, and P. James. 2007. Methods for the detection and analysis of protein-protein interactions. *Proteomics.* 7:2833–2842.
4. Behnen, P., E. Davis, …, S. Linse. 2012. Calcium-dependent interaction of calmodulin with human 80S ribosomes and polyribosomes. *Biochemistry.* 51:6718–6727.
5. Guilliams, T., F. El-Turk, …, E. De Genst. 2013. Nanobodies raised against monomeric α-synuclein distinguish between fibrils at different maturation stages. *J. Mol. Biol.* 425:2397–2411.
6. Paslawski, W., S. Mysling, …, D. E. Otzen. 2014. Co-existence of two different α-synuclein oligomers with different core structures determined by hydrogen/deuterium exchange mass spectrometry. *Angew. Chem. Int. Ed. Engl.* 53:7560–7563.
7. Jecklin, M. C., S. Schauer, …, R. Zenobi. 2009. Label-free determination of protein-ligand binding constants using mass spectrometry and validation using surface plasmon resonance and isothermal titration calorimetry. *J. Mol. Recognit.* 22:319–329.
8. Abate, A. R., T. Hung, …, D. A. Weitz. 2010. High-throughput injection with microfluidics using picoinjectors. *Proc. Natl. Acad. Sci. USA.* 107:19163–19166.
9. Song, Y., Z. Liu, …, H. C. Shum. 2013. Manipulation of viscous all-aqueous jets by electrical charging. *Chem. Commun. (Camb.).* 49: 1726–1728.
10. Wienken, C. J., P. Baaske, …, S. Duhr. 2010. Protein-binding assays in biological liquids using microscale thermophoresis. *Nat. Commun.* 1:100.
11. Hannig, K. 1961. Die trägerfreie kontinuierliche Elektrophorese und ihre Anwendung. *Anal. Chem.* 181:244–254.
12. Harrison, D. J., A. Manz, …, H. M. Widmer. 1992. Capillary electrophoresis and sample injection systems integrated on a planar glass chip. *Anal. Chem.* 64:1926–1932.
13. Raymond, D. E., A. Manz, and H. M. Widmer. 1994. Continuous sample pretreatment using a free-flow electrophoresis device integrated onto a silicon chip. *Anal. Chem.* 66:2858–2865.
14. Carbeck, J. D., I. J. Colton, …, G. M. Whitesides. 1998. Protein charge ladders, capillary electrophoresis, and the role of electrostatics in biomolecular recognition. *Acc. Chem. Res.* 31:343–350.
15. Herling, T. W., T. Müller, …, T. P. J. Knowles. 2013. Integration and characterization of solid wall electrodes in microfluidic devices fabricated in a single photolithography step. *Appl. Phys. Lett.* 102:184102.
16. Herling, T. W., P. Arosio, …, T. P. J. Knowles. 2015. A microfluidic platform for quantitative measurements of effective protein charges and single ion binding in solution. *Phys. Chem. Chem. Phys.* 17:12161–12167.
17. Köhler, S., C. Weilbeer, …, D. Belder. 2011. PDMS free-flow electrophoresis chips with integrated partitioning bars for bubble segregation. *Lab Chip.* 11:309–314.
18. Turgeon, R. T., B. R. Fonslow, …, M. T. Bowser. 2010. Measuring aptamer equilibria using gradient micro free flow electrophoresis. *Anal. Chem.* 82:3636–3641.
19. Berridge, M. J., P. Lipp, and M. D. Bootman. 2000. The versatility and universality of calcium signalling. *Nat. Rev. Mol. Cell Biol.* 1:11–21.
20. Clapham, D. E. 2007. Calcium signaling. *Cell.* 131:1047–1058.
21. O'Connell, D. J., M. C. Bauer, …, D. J. Cahill. 2010. Integrated protein array screening and high throughput validation of 70 novel neural calmodulin-binding proteins. *Mol. Cell. Proteomics.* 9:1118–1132.
22. Kuboniwa, H., N. Tjandra, …, A. Bax. 1995. Solution structure of calcium-free calmodulin. *Nat. Struct. Biol.* 2:768–776.
23. Babu, Y. S., C. E. Bugg, and W. J. Cook. 1988. Structure of calmodulin refined at 2.2 A resolution. *J. Mol. Biol.* 204:191–204.
24. Kretsinger, R. H., and C. E. Nockolds. 1973. Carp muscle calcium-binding protein. II. Structure determination and general description. *J. Biol. Chem.* 248:3313–3326.
25. Linse, S., C. Johansson, …, S. Forsén. 1991. Electrostatic contributions to the binding of Ca^{2+} in calbindin D9k. *Biochemistry.* 30:154–162.
26. Priddy, T. S., C. R. Middaugh, and G. M. Carlson. 2007. Electrostatic changes in phosphorylase kinase induced by its obligatory allosteric activator Ca^{2+}. *Protein Sci.* 16:517–527.
27. Meador, W. E., A. R. Means, and F. A. Quiocho. 1992. Target enzyme recognition by calmodulin: 2.4 A structure of a calmodulin-peptide complex. *Science.* 257:1251–1255.
28. Ikura, M., G. M. Clore, …, A. Bax. 1992. Solution structure of a calmodulin-target peptide complex by multidimensional NMR. *Science.* 256:632–638.
29. Clapperton, J. A., S. R. Martin, …, P. M. Bayley. 2002. Structure of the complex of calmodulin with the target sequence of calmodulin-

dependent protein kinase I: studies of the kinase activation mechanism. *Biochemistry.* 41:14669–14679.

30. Aoyagi, M., A. S. Arvai, …, E. D. Getzoff. 2003. Structural basis for endothelial nitric oxide synthase binding to calmodulin. *EMBO J.* 22:766–775.
31. Cook, A. G., L. N. Johnson, and J. M. McDonnell. 2005. Structural characterization of Ca^{2+}/CaM in complex with the phosphorylase kinase PhK5 peptide. *FEBS J.* 272:1511–1522.
32. Yamniuk, A. P., and H. J. Vogel. 2004. Calmodulin's flexibility allows for promiscuity in its interactions with target proteins and peptides. *Mol. Biotechnol.* 27:33–57.
33. Junker, J. P., F. Ziegler, and M. Rief. 2009. Ligand-dependent equilibrium fluctuations of single calmodulin molecules. *Science.* 323: 633–637.
34. Stigler, J., F. Ziegler, …, M. Rief. 2011. The complex folding network of single calmodulin molecules. *Science.* 334:512–516.
35. Wallimann, T., M. Wyss, …, H. M. Eppenberger. 1992. Intracellular compartmentation, structure and function of creatine kinase isoenzymes in tissues with high and fluctuating energy demands: the "phosphocreatine circuit" for cellular energy homeostasis. *Biochem. J.* 281:21–40.
36. Bong, S. M., J. H. Moon, …, K. Y. Hwang. 2008. Structural studies of human brain-type creatine kinase complexed with the ADP-Mg^{2+}-NO^{3-}-creatine transition-state analogue complex. *FEBS Lett.* 582: 3959–3965.
37. Christakos, S. 2012. Mechanism of action of 1,25-dihydroxyvitamin D3 on intestinal calcium absorption. *Rev. Endocr. Metab. Disord.* 13:39–44.
38. Brostrom, C. O., F. L. Hunkeler, and E. G. Krebs. 1971. The regulation of skeletal muscle phosphorylase kinase by Ca^{2+}. *J. Biol. Chem.* 246:1961–1967.
39. Cohen, P., A. Burchell, …, C. Nairn. 1978. Identification of the Ca^{2+}-dependent modulator protein as the fourth subunit of rabbit skeletal muscle phosphorylase kinase. *FEBS Lett.* 92:287–293.
40. McDonald, J. C., and G. M. Whitesides. 2002. Poly(dimethylsiloxane) as a material for fabricating microfluidic devices. *Acc. Chem. Res.* 35:491–499.
41. Spiga, M., and G. L. Morino. 1994. A symmetric solution for velocity profile in laminar flow through rectangular ducts. *Int. Commun. Heat Mass Transfer.* 21:469–475.
42. Delaglio, F., S. Grzesiek, …, A. Bax. 1995. NMRPipe: a multidimensional spectral processing system based on UNIX pipes. *J. Biomol. NMR.* 6:277–293.
43. So, J.-H., and M. D. Dickey. 2011. Inherently aligned microfluidic electrodes composed of liquid metal. *Lab Chip.* 11:905–911.
44. Hellstrand, E., S. Kukora, …, K. S. Åkerfeldt. 2013. Förster resonance energy transfer studies of calmodulin produced by native protein ligation reveal inter-domain electrostatic repulsion. *FEBS J.* 280:2675–2687.
45. Bottomley, P. A., G. S. Panjrath, …, R. G. Weiss. 2013. Metabolic rates of ATP transfer through creatine kinase (CK Flux) predict clinical heart failure events and death. *Sci. Transl. Med.* 5:215re3.
46. Linse, S., B. Jönsson, and W. J. Chazin. 1995. The effect of protein concentration on ion binding. *Proc. Natl. Acad. Sci. USA.* 92:4748–4752.
47. Watterson, D. M., F. Sharief, and T. C. Vanaman. 1980. The complete amino acid sequence of the Ca^{2+}-dependent modulator protein (calmodulin) of bovine brain. *J. Biol. Chem.* 255:962–975.
48. Lund, M., and B. Jönsson. 2013. Charge regulation in biomolecular solution. *Q. Rev. Biophys.* 46:265–281.
49. Berg, J. M., J. L. Tymoczko, and L. Stryer. 2010. Biochemistry, 7th ed. W. H. Freeman, New York.
50. Jiao, M., H. T. Li, …, Y. Liang. 2010. Attractive protein-polymer interactions markedly alter the effect of macromolecular crowding on protein association equilibria. *Biophys. J.* 99:914–923.
51. Yuan, T., M. P. Walsh, …, H. J. Vogel. 1999. Calcium-dependent and -independent interactions of the calmodulin-binding domain of cyclic nucleotide phosphodiesterase with calmodulin. *Biochemistry.* 38:1446–1455.
52. Waltersson, Y., S. Linse, …, T. Grundström. 1993. Mutational effects on the cooperativity of Ca^{2+} binding in calmodulin. *Biochemistry.* 32:7866–7871.
53. Meyer, W. L., E. H. Fischer, and E. G. Krebs. 1964. Activation of skeletal muscle phosphorylase b kinase by Ca^{2+}*. *Biochemistry.* 3:1033–1039.

Biophysical Journal, Volume *110*

Supplemental Information

A Microfluidic Platform for Real-Time Detection and Quantification of Protein-Ligand Interactions

Therese W. Herling, David J. O'Connell, Mikael C. Bauer, Jonas Persson, Ulrich Weininger, Tuomas P.J. Knowles, and Sara Linse

Biophysical Journal

Supporting Material

A Microfluidic Platform for Real-Time Detection and Quantification of Protein-Ligand Interactions

Therese W. Herling,[1] David J. O'Connell,[2] Mikael C. Bauer,[3] Jonas Persson,[3,5] Ulrich Weininger,[4] Tuomas P. J. Knowles,[1,*] and Sara Linse[3,*]

[1]Department of Chemistry, University of Cambridge, Cambridge, United Kingdom; [2]School of Biomolecular and Biomedical Science, University of College Dublin, Dublin, Ireland; [3]Department of Biochemistry and Structural Biology and [4]Department of Biophysical Chemistry, Lund University, Lund, Sweden; and [5]Department of Immunology, Genetics and Pathology, Uppsala University, Uppsala, Sweden.

*Correspondence: tpjk2@cam.ac.uk; sara.linse@biochemistry.lu.se

Supporting Material for: A microfluidic platform for real-time detection and quantification of protein-ligand interactions

T.W. Herling[1], D.J. O'Connell[2], M.C. Bauer[3], J. Persson[3], U. Weininger[4], T.P.J. Knowles[1], S. Linse[3]

[1]Department of Chemistry, University of Cambridge, CB2 1EW Cambridge, UK. [2]School of Biomolecular and Biomedical Science, University College Dublin, Dublin 4, Ireland. [3]Department of Biochemistry and Structural Biology, Lund University, 22100 Lund, Sweden. [4]Department of Biophysical Chemistry, Lund University, 22100 Lund, Sweden.

Expression and purification of calmodulin

Full length human calmodulin was expressed from a modified Pet3a vector ('PetSac' with NdeI and SacI cloning sites) containing a synthetic calmodulin gene. The wild-type gene was built with the codons preferred by *Escherichia coli*(1). The calmodulin gene with mutation S17C was amplified by polymerase chain reaction (PCR) from this vector using primers containing the desired base change in two steps using standard procedures. The PCR product was digested by NdeI and SacI and cloned into the PetSac vector.

Following transformation, the mutant protein was expressed in *E. coli* strain BL21(De3)pLysS star in LB medium and the wild-type protein was purified using heat treatment, anion exchange chromatography, hydrophobic interaction chromatography and gel filtration. The purification started with sonication of cell pellet from 4.5 litre culture in a total of 100 mL 20 mM Tris-HCl, 1 mM $CaCl_2$, 1 mM DTT, 20 mM NaCl, pH 7.5 (buffer A). Two portions of 50 mL were sonicated for 1.5 minutes each using a tip sonicator (1/2 horn, maximum output, duty cycle 50%) in a beaker surrounded by ice-water slurry. The sonicates were centrifuged at 18,000 rcf for 10 minutes at $4^{\circ}\mathrm{C}$ (spin 1). The supernatant was poured into 100 mL boiling buffer A and heated to 85°C to precipitate *E. coli* proteins, followed by rapid cooling (beaker gently swirled in surrounding ice-water slurry) and centrifugation at 18,000 rcf for 10 minutes at $4^{\circ}\mathrm{C}$ (spin 2). The supernatant from spin 2 was pumped onto a 5.4 x 12 cm DEAE cellulose column packed and equilibrated in buffer A. The pellet from spin 1 was sonicated in 40 mL of buffer A, centrifuged (spin 3), heat treated and centrifuged (spin 4) as above. The supernatant from spin 4 was loaded onto the same DEAE cellulose column as above. The column was washed with 200 mL buffer A and eluted by a linear gradient from 20 - 500 mM NaCl in 20 mM Tris-HCl, 1 mM $CaCl_2$, 1 mM DTT, pH 7.5, total gradient volume 1200 mL. 10 mL fractions were collected and examined by agarose gel electrophoresis. Fractions containing calmodulin, total volume 650 mL, were pumped onto a 5.4 x 14 cm phenyl sepharose column equilibrated in 50 mM Tris-HCl, 1 mM $CaCl_2$, 1 mM DTT, 150 mM NaCl, pH 7.5. The column was washed with 300 mL of 50 mM Tris-HCl, 1 mM $CaCl_2$, 1 mM DTT, 150 mM NaCl, pH 7.5, followed by elution with 500 mL 50 mM Tris-HCl, 1 mM EDTA, 1 mM DTT, 150 mM NaCl, pH 7.5. 8 mL fractions were collected and examined by UV absorbance at 280 nm, SDS PAGE and agarose gel electrophoresis. Fractions containing calmodulin were combined and lyophilised, followed by desalting on a 3.4 x 20 cm Sephadex G25 superfine column in water through a zone of decalcified NaCl. This resulted in Ca^{2+}-free (apo) calmodulin, which was also free from the EDTA used to chelate Ca^{2+}. The G25 column was first washed with EDTA, pH 7,5, and then Millipore water. 5 mL of saturated NaCl, pH 7.5 (stored in a plastic flask containing 5 ml Chelex resin in a dialysis bag; the dialysis tubing was boiled four times in Millipore water before filling with Chelex resin equilibrated to pH 7.5) was applied to the column directly before the calmodulin sample was applied. The protein was eluted in water and 3 mL fractions collected in plastic tubes, examined by UV absorbance at 280 nm, and lyophilised. This procedure was repeated three times with a third of the protein being desalted in each repeat. The final yield was 770 mg pure apo-calmodulin-S17C, based on the weight of the lyophilised powder.

The purity at protein level was confirmed by agarose gel electrophoresis in EDTA and in Ca^{2+}, and by SDS-polyacrylamide gel electrophoresis. The absence of EDTA and other small molecules was confirmed by ^{1}H NMR spectroscopy. Titrations in the presence of Quin2 were used to quantify the residual Ca^{2+} concentration in the apo protein sample, and found to be less than 0.04 molar equivalents, which is less than 1% of full saturation.

0006-3495/08/09/2624/12 $2.00 doi: xx.xxxx/biophysj.xxx.xxxxxx

Alexa labelling

Calmodulin-S17C was labeled with the fluorescent dye Alexa546 for ProtoArray screening or with Alexa488 for the microfluidic studies. 10 mg calmodulin was dissolved in 20 mM phosphate buffer with 100 mM NaCl, 1 mM EDTA, 1 mM DTT, pH 7.3, incubated for one hour and DTT removed by gel filtration on a NAP-10 column in 20 mM phosphate buffer with 100 mM NaCl, and 1 mM EDTA, pH 7.3 One molar equivalent of Alexa546 C5-maleimide (Invitrogen, California, US) or with Alexa488 C5-maleimide (Invitrogen, California, US) was added and the labelling mixture was then left to react at room temperature in the dark for one hour. Excess unbound dye was removed by passing the reaction twice through a NAP-10 size exclusion column (washed with 5 mL 1 mM EDTA, pH 7,5, and then 15 mL Millipore water, with water as the eluent and collecting the protein fraction. The labelled protein was immediately divided into aliquots and frozen.

Protein array screen

A protein array screen was performed to probe for potential calmodulin binding partners as described in the main text and methods section. In the analysis, Alexa546 labelled calmodulin binding to immobilised protein spots on these arrays targets were recorded, we used a signal intensity above a cutoff of 200. The calmodulin target proteins identified in this screen are shown in SI Fig. 1 and 2. SI Fig. 1 contains the proteins identified in the presence of free Ca^{2+}. The proteins highlighted in bold font were only identified in the presence of calcium ions.

The proteins targeted by calmodulin in the absence of free Ca^{2+} are listed in SI Fig. 2. Systems that were only above the signal intensity threshold for apo-calmodulin are shown in bold font.

Surface plasmon resonance studies

All SPR experiments were carried out using a Biacore 3000 instrument. S17C calmodulin was immobilised using ligand thiol disulphide exchange coupling, following the procedures recommended by the supplier (GE Healthcare). The dextran matrix of a CM5 chip was activated by injecting 25 μL of a fresh mixture of 0.05 M N-hydroxysuccimide, and 0.2 M 1-ethyl-3-(3-dimethylaminopropyl)carbodiimide. A reactive disulphide group was then introduced on the sensor chip surface by injecting 20 μL of 100 μM 2-(2-pyridinyldithio)ethaneamine, PDEA, 0.1 M sodium borate, pH 8.5. Calmodulin was then immobilised by injecting 100 μL of 10 μg/mL calmodulin S17C in 10 mM HCO_2Na (sodium formate), pH 4.3. Finally, residual PDEA groups were deactivated by injecting 40 μL of 50 mM L-cysteine, 1 M NaCl, 100 mM HCO_2Na, pH 4.3. Blank channels for negative control were prepared by omitting calmodulin in the coupling step, and an additional control channel was prepared by immobilisation of human serum albumin. Binding of targets was surveyed by injecting 150 μL of creatine kinase solutions in 10 mM Tris-HCl, 150 mM KCl, 1 mM $CaCl_2$, 0.005% v/v Tween20, pH 7.5. Dissociation of target protein from calmodulin was followed under buffer flow. The chip was then regenerated by injecting 100 μL of 1 M NaCl, 10 mM glycine, pH 2.5. The flow rate was 10 μL/min throughout the experiment. For an SPR experiment, where the expected K_d is on the order of micromolar, 100 picomoles of material would be required for the immobilisation step (100 μL of 1 μM solution). An additional 10 - 200 picomoles of free protein for injection would be consumed depending on the kinetics of binding and dissociation.

The rate constants were obtained by fitting a single exponential decay to the dissociation data after baseline subtraction, right panels in Fig. 2B and SI Fig. 3, using the response, R, as a function of time, t,

$$R(t) = A\, e^{-k_{\rm off} t}, \tag{1}$$

with the variable parameters being the dissociation rate constant, $k_{\rm off}$, and the amplitude of the signal, A. The association phase data, left panels in Fig. 2B and SI Fig. 3, were analysed by fitting the following function:

$$R(t) = R_{\rm max}\, \frac{c k_{\rm on}}{k_{\rm off} + c\, k_{\rm on}} \left(1 - e^{-(k_{\rm off} + c k_{\rm on})t}\right) R_0, \tag{2}$$

using the $k_{\rm off}$ determined with equation 1 and the protein concentration, c. The variable parameters were: the association rate constant, $k_{\rm on}$; the signal at full saturation of all the immobilised targets, $R_{\rm max}$; and the response resulting from the injection of the protein, R_0. The resulting rates constants were $k_{\rm on} = 7.3 \times 10^2\ {\rm M^{-1}s^{-1}}$, $k_{\rm off} = 2.6 \times 10^{-5}\ {\rm s^{-1}}$ for creatine kinase B in the presence of Ca^{2+}. Relating the rate constants to the equilibrium dissociation constant, K_d, through

$$K_d = \frac{k_{\rm off}}{k_{\rm on}} \tag{3}$$

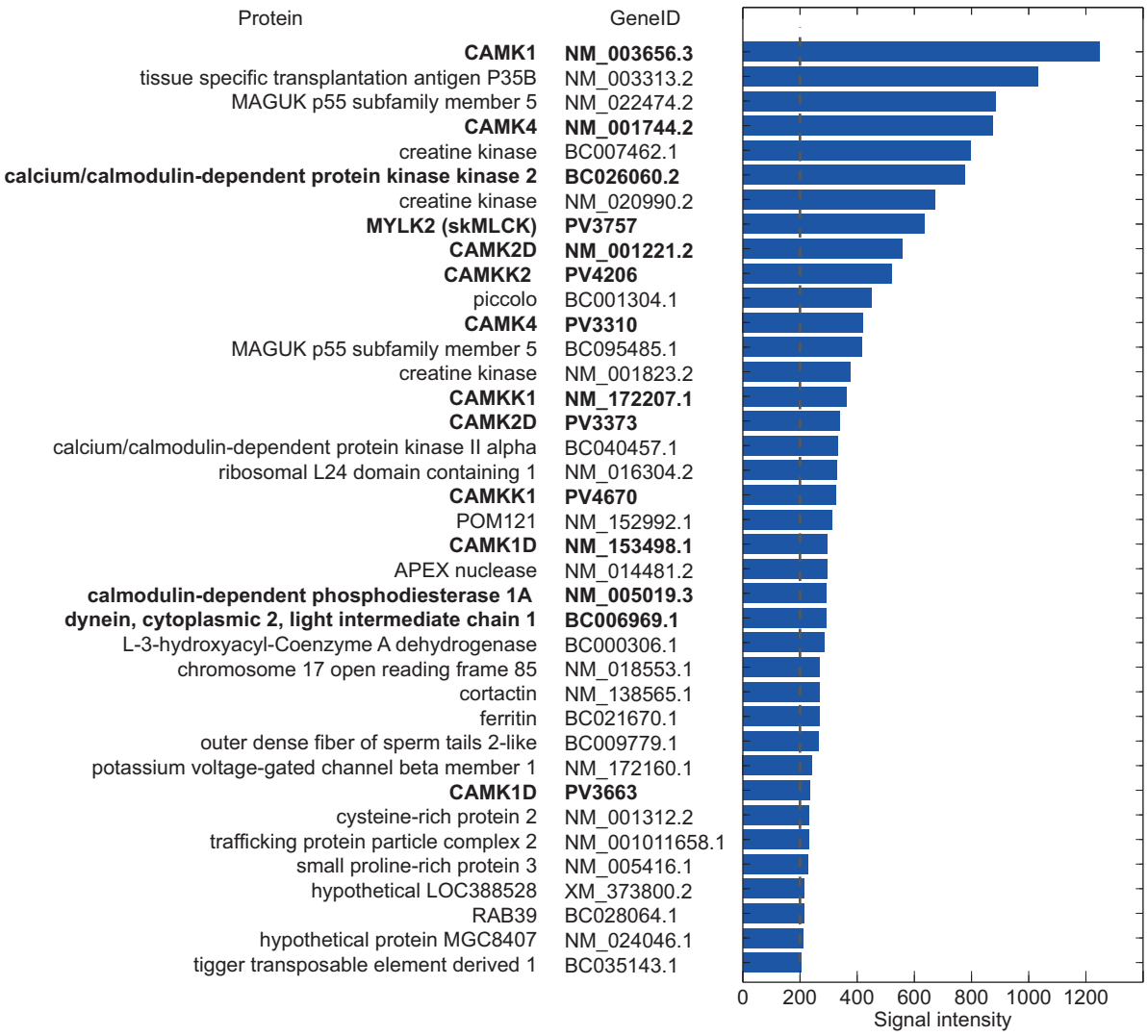

Figure 1: Putative calmodulin targets identified in the ProtoArray screen in the presence of Ca^{2+}. Targets in bold are identified in the presence of Ca^{2+} only.

results in values for the equilibrium dissociation constant of $K_d = 36$ nM for calmodulin binding to creatine kinase B on the sensor chip surface.

Further to the free flow electrophoresis measurements described below, the calcium dependence of the interaction between calmodulin and phosphorylase kinase was also investigated by SPR, SI Fig. 3. In the presence of added Ca^{2+}, rabbit phosphorylase kinase was observed to bind to immobilised calmodulin with a very low dissociation rate. Only limited dissociation was observed over the course of days, as discussed in the main text the slow dissociation of phosphorylase kinase may be due to avidity effects. In the presence of EDTA to chelate any trace Ca^{2+}, we did not observe any binding of phosphorylase kinase to the immobilised calmodulin. The data shown in magenta in SI Fig. 3 has therefore been normalised against the maximum response in the calcium buffer.

In the case of phosphorylase kinase we only observed binding to calmodulin in the presence of Ca^{2+}, SI Fig. 3. Fitting this data as described above resulted in $k_{\mathrm{on}} = 3.1 \times 10^4$ M^{-1} s^{-1} and $k_{\mathrm{off}} = 1 \times 10^{-6}$ s^{-1}. As mentioned in the Discussion section, the very low observed k_{off} could be an artefact due to binding of one multimeric phosphorylase kinase to multiple immobilised copies of calmodulin. In this situation phosphorylase kinase would be required to dissociate simultaneously from up to four copies of calmodulin before leaving the surface of the chip.

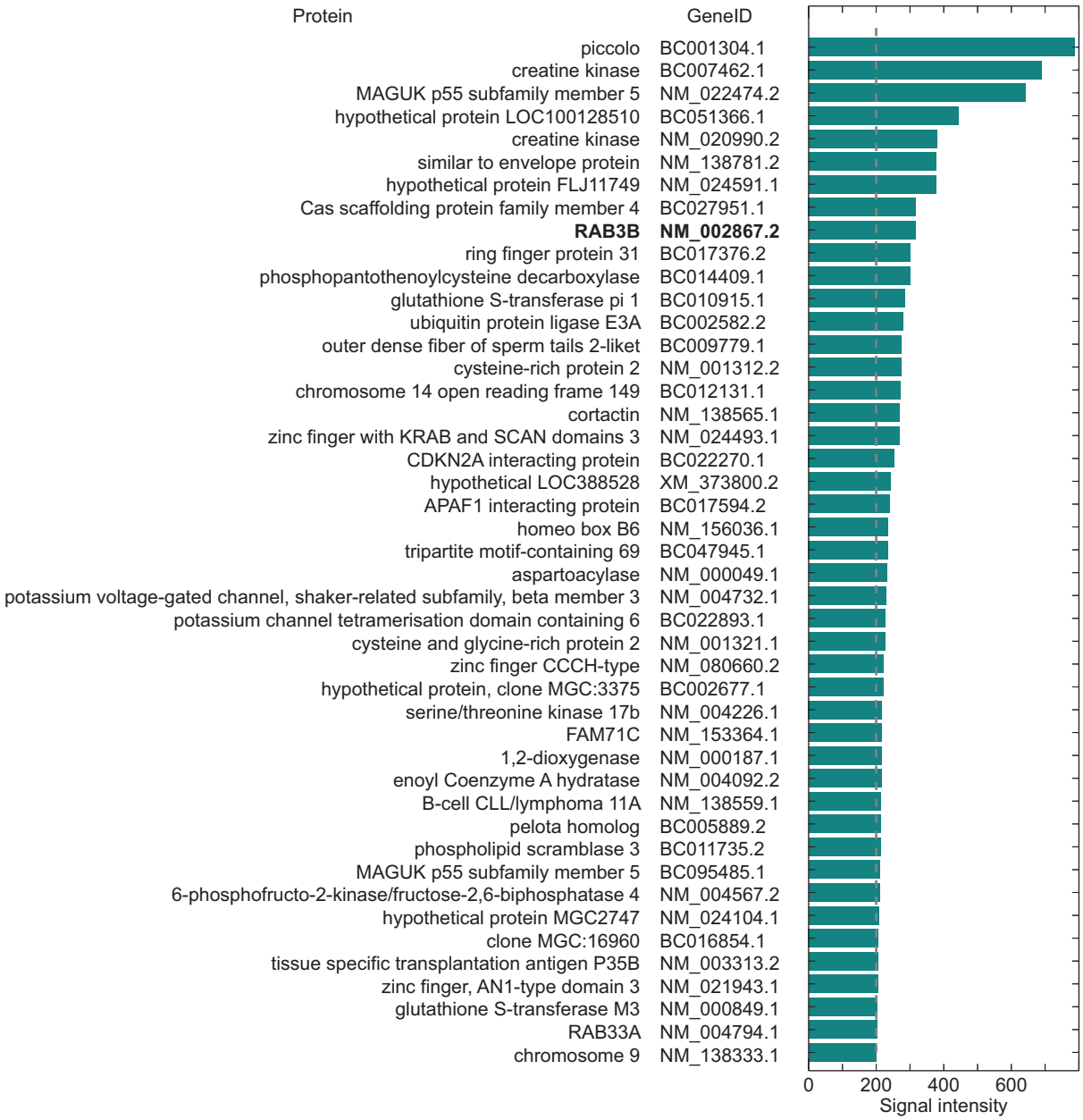

Figure 2: Putative calmodulin targets identified in the ProtoArray screen in the absence of Ca^{2+}. Targets in bold are identified in the absence of Ca^{2+} only.

Microfluidic device preparation

Microfluidic devices were cast in PDMS (Sylgard 184, Dow Corning, Onecall, UK) using standard soft lithography methods(2). The clear PDMS was coloured black by the addition of a small quantity of carbon nanopowder, 0.2% w/w, prior to curing (Sigma, UK). Inlet and outlet holes were punched using a biopsy punch (WPI, Florida, US). The PDMS devices were bonded to glass slides in a plasma oven using an oxygen plasma (Diener Electronics, Germany). The electrodes were fabricated by placing the bonded device glass slide down on a hot plate set to 79°C and inserting InBiSn alloy (51% In, 32.5% Bi, 16.5% Sn, Conro Electronics, UK) through the solder inlet, Fig. 1A. The electrodes were automatically aligned with the fluidic channel by an array of micropillars. These pillars defined the border between fluidic and solder channels, whilst maintaining direct contact between the liquid and the metal electrodes.

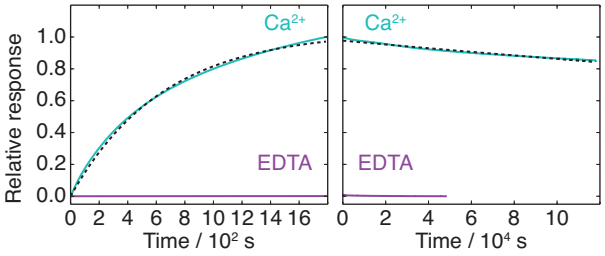

Figure 3: SPR measurements. Interaction between phosphorylase kinase and immobilised calmodulin. Left: association of phosphorylase kinase in the presence of Ca^{2+} in cyan, with the fit represented by the dashed line. The magenta line shows the signal in the presence of EDTA. No binding was detected in the absence of Ca^{2+}, the data in EDTA has therefore been normalised to the maximum signal in the calcium buffer. The dissociation data is shown in the right panel.

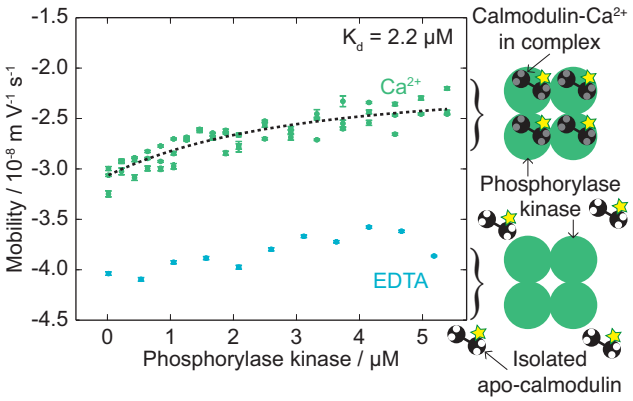

Figure 4: Calmodulin and phosphorylase kinase. (a) The observed electrophoretic mobility of calmodulin in response to an increasing concentration of phosphorylase kinase, in the presence of either 0.1 mM $CaCl_2$ (green) or 0.1 mM EDTA (blue).

Electrophoresis experiments

Electrophoresis experiments were performed in the type of microfluidic device seen in Fig. 1. Binding curves for calmodulin-target protein interactions were obtained by investigating samples containing a fixed concentration of Alexa488 labelled calmodulin and a varying concentration of target protein. The concentration ranges investigated were adjusted so as to reach a plateau in the observed electrophoretic mobility. In the case of phosphorylase kinase the solubility of the target protein was also a consideration.

Four repeats of a voltage range at set increments were performed for each protein concentration. Three images and current readings were obtained at each voltage step, Fig. 3. The voltage range and increments were adjusted to achieve considerable sample deflection, and thereby a relatively low error on δ, whilst avoiding the accumulation of electrolysis products at the electrode interfaces.

For a 1:1 interaction between calmodulin, C, and the target protein binding sites, P, with the total concentrations of C_t and P_t, K_d can be determined from the observed electrophoretic mobility, if there is a difference between the mobility of C and the complex, CP.

$$K_d = \frac{[\mathrm{C}] \cdot [\mathrm{P}]}{[\mathrm{CP}]} = \frac{[\mathrm{C}] \cdot (\mathrm{P_t} - \mathrm{C_t} + [\mathrm{C}])}{\mathrm{C_t} - [\mathrm{C}]}, \tag{4}$$

The observed electrophoretic mobility is the weighted sum of the fractional contributions from the mobilities of the isolated calmodulin, μ_c, and bound calmodulin, μ_{cp}

$$\mu_{obs} = \mu_c \frac{[\mathrm{C}]}{\mathrm{C_t}} + \mu_{\mathrm{cp}} \frac{[\mathrm{CP}]}{\mathrm{C_t}}, \tag{5}$$

the quadratic equation, Eqn. 6, was solved for [C].

$$0 = [\mathrm{C}]^2 + (K_d + \mathrm{P_t} - \mathrm{C_t}) \cdot [\mathrm{C}] - K_d \cdot \mathrm{C_t} \tag{6}$$

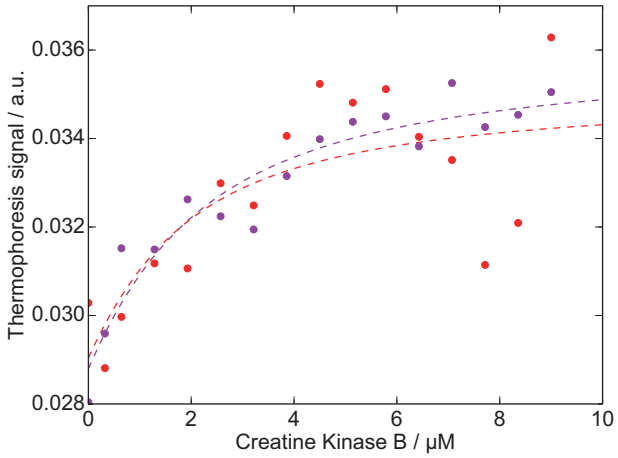

Figure 5: Thermophoresis experiments with calmodulin and creatine kinase B. The binding of 1 μM Alexa488-labelled calmodulin to creatine kinase B was monitored by thermophoresis. The experiments were carried out in a low ionic strength buffer: 0.1 mM $CaCl_2$, 5 mM Tris-HCl pH 8.0 (red) and in a high salt buffer: 150 mM KCl, 0.1 mM $CaCl_2$, 5 mM Tris-HCl pH 8.0 (magenta). Fits to the thermophoresis signal resulted in $K_d = 1.4$ μM for the low ionic strength buffer (red line) and $K_d = 1.7$ μM for the measurements at high salt concentrations (magenta line).

The resulting expression for [C] in terms of $\mathrm{P_t}$, $\mathrm{C_t}$, and K_d is shown below in equation 7.

$$[\mathrm{C}] = \mu_\mathrm{c} \frac{(-\mathrm{P_t} + \mathrm{C_t} - K_d + \sqrt{(\mathrm{P_t} - \mathrm{C_t} + K_d)^2 + 4K_d\mathrm{C_t}})}{2}. \tag{7}$$

By combining equations 7 and 5, we were able to fit the free flow electrophoresis data to obtain the equilibrium dissociation constants for the interactions investigated in this study. The two concentrations $[\mathrm{P_t}]$ and $[\mathrm{C_t}]$ were known experimental parameters, leaving μ_c μ_cp, and K_d as the fitting parameters.

Free flow electrophoresis with a known binding partner

In a set of positive control experiments, we evaluated the use of free flow electrophoresis to detect and characterise the binding of calmodulin to phosphorylase kinase, a well-documented ligand(3, 4). The activation of phosphorylase kinase in response to an increase in the intracellular Ca^{2+} concentration during muscle contraction leads to glycogenolysis(4–7). Phosphorylase kinase is a large, 1.3 MDa, hexadecameric complex, consisting of four repeats of its $\alpha\beta\gamma\delta$ subunits, each protein complex thus has four calmodulin binding sites. The δ subunit is an auto regulatory calmodulin homologue, it binds and activates the catalytic γ subunit in response to Ca^{2+}(3, 4).

We measured the electrophoretic mobilities of samples containing 1 μM calmodulin and 0 - 5.2 μM phosphorylase kinase $\alpha\beta\gamma\delta$ subunit in 5 mM Tris-HCl pH 8, 0.1 mM $CaCl_2$ by free flow electrophoresis, Fig. 4. In complementary experiments we also investigated the binding of 1 μM apo-calmodulin to phosphorylase kinase (0 to 5.0 μM $\alpha\beta\gamma\delta$) in 5 mM Tris-HCl pH 8 containing 0.1 mM EDTA to chelate any residual Ca^{2+}.

By measuring the change in electrophoretic mobility we were able to monitor the binding equilibrium between calmodulin and phosphorylase kinase in the presence of Ca^{2+}, green points in Fig. 4. In the absence of free Ca^{2+} we did not observe a monotonic change in the μ_obs for calmodulin, cyan points in Fig. 4, indicating a lack of interaction between the two proteins in the absence of free calcium ions. In agreement with the findings from the free flow electrophoresis experiments, when we performed SPR experiments investigating the binding of phosphorylase kinase to immobilised calmodulin, binding was only observed in the presence of free Ca^{2+}, see SI Fig. 3.

Thermophoresis

Thermophoresis experiments were conducted in 5 mM Tris-HCl pH 8.0, 0.1 mM $CaCl_2$ and either 0 mM or 150 mM KCl. Sixteen samples were prepared in each buffer with 1 μM Alexa488-calmodulin and creatine kinase B concentrations , $\mathrm{C_{CKB}}$

ranging from 0 to 9 μM, Fig. 5. The samples were placed in low-binding capillaries (MST Premium Coated from Nanotemper Technologies, Germany) and mounted in a Monolith NT.115 Instrument (Nanotemper Technologies, Germany) operated at 25°C. Thermophoresis measurements were performed using LED power 20% and themorophoresis 50% for 25 s. The thermophoresis signal, as a function of total creatine kinase B concentration, C, in μM, was fitted using a 1:1 binding equation:

$$\mathrm{Y} = \mathrm{Y}_{\mathrm{free}} + \mathrm{Y}_{\mathrm{bound}} \cdot \frac{\mathrm{X}}{\mathrm{X} + K_d} \tag{8}$$

where

$$\mathrm{X} = -0.5 \cdot (K_d + 1.0 - \mathrm{C}_{\mathrm{CKB}}) + \sqrt{0.25 \cdot (K_d + 1.0 - \mathrm{C}_{\mathrm{CKB}})^2 + \mathrm{C}_{\mathrm{CKB}} \cdot K_d} \tag{9}$$

where Y is calculated signal, $\mathrm{Y}_{\mathrm{free}}$ its contribution from free Alexa488-calmodulin and $\mathrm{Y}_{\mathrm{bound}}$ its contribution from Alexa488-calmodulin bound to creatine kinase B. X is the free creatine kinase B concentration, $\mathrm{C}_{\mathrm{CKB}}$ the total creatine kinase B concentration in μM, 1.0 is the total Alexa488-calmodulin concentration in μM. Fits to the thermophoresis signal resulted in K_d = 1.4 μM for the low ionic strength buffer and K_d = 1.7 μM for the measurements at high salt concentrations, see Fig. 5.

References

1. Waltersson, Y., S. Linse, P. Brodin, and T. Grundström, 1993. Mutational effects on the cooperativity of Ca2+ binding in calmodulin. Biochemistry 32:7866–7871.
2. McDonald, J. C., and G. M. Whitesides, 2002. Poly (dimethylsiloxane) as a material for fabricating microfluidic devices. Acc. Chem. Res. 35:491–499.
3. Cohen, P., A. Burchell, J. Foulkes, P. T. W. Cohen, T. C. Vanaman, and A. C. Nairn, 1978. Identification of the Ca2+-dependent modulator protein as the fourth subunit of rabbit skeletal muscle phosphorylase kinase. FEBS Lett. 92:287–293.
4. Cook, A. G., L. N. Johnson, and J. M. McDonnell, 2005. Structural characterization of Ca2+/CaM in complex with the phosphorylase kinase PhK5 peptide. FEBS J. 272:1511–1522.
5. Meyer, W. L., E. H. Fischer, and E. G. Krebs, 1964. Activation of Skeletal Muscle Phosphorylase b Kinase by CA2+ *. Biochemistry 3:1033–1039.
6. Brostrom, C. O., F. L. Hunkeler, and E. G. Krebs, 1971. The Regulation of Skeletal Muscle Phosphorylase Kinase by Ca2+. J. Biol. Chem. 246:1961–1967.
7. Priddy, T. S., C. R. Middaugh, and G. M. Carlson, 2007. Electrostatic changes in phosphorylase kinase induced by its obligatory allosteric activator Ca2+. Prot. Sci. 16:517–527.